Available online at www.sciencedirect.com

ScienceDirect

Procedia Structural Integrity 23 (2019) 378–383

Structural Integrity Procedia

www.elsevier.com/locate/procedia

9th International Conference on Materials Structure and Micromechanics of Fracture

Influence of isothermal oxidation on microstructure of YSZ and Mullite-YSZ thermal barrier coatings

David Jech[a]*, Ladislav Čelko[a], Michaela Remešová[a], Karel Slámečka[a], Pavel Ctibor[b]

[a]CEITEC – Central European Institute of Technology, Brno University of Technology, Purkyňova 123, 612 00 Brno, Czech Republic
[b]IPP – Institute of Plasma Physics, Academy of Sciences of the Czech Republic, Za Slovankou 3, 182 00 Prague, Czech Republic

Abstract

Microstructural changes in conventional yttria stabilized zirconia (YSZ) and multilayer Mullite-YSZ/YSZ (M-YSZ) thermal barrier coatings were compared based on high temperature isothermal oxidation at the temperatures of 1050, 1150 and 1250 °C. Both types of thermal barrier coatings were produced from commercially available powders utilizing atmospheric plasma spray technique. Initial M-YSZ powder mixture consisted of 29 vol. % of Mullite and 71 vol. % of YSZ. Inconel Alloy 713LC nickel-based superalloy was used as a substrate material (cylinders, 25 mm in diameter and 10 mm in thickness). The TBCs lifetime, phase stability, thickness of the thermally grown oxide layer, porosity, and changes in microstructure after high temperature testing were evaluated using light microscope, scanning electron microscope equipped with EDX analyzer, and XRD technique.

Keywords: Atmospheric plasma spraying; Thermal barrier coatings; Isothermal oxidation; Microstructure; Thermally grown oxide;

1. Introduction

Complex material systems of thermal barrier coatings are nowadays the most effective protection of high temperature exposed components in land-based turbines and jet engines. Aircraft turbine blades and combustion chambers are usually exposed to long term high temperature oxidation and corrosion during operation. Operating temperature inside the combustion chamber is proportional to engine efficiency and inversely proportional to overall fuel consumption and undesirable production of CO_2. Therefore, a considerable effort has recently been devoted to

* Corresponding author. Tel.: +420 54114 9892.
E-mail address: david.jech@ceitec.vutbr.cz

2452-3216
10.1016/j.prostr.2020.01.116

research and development of new types of ceramic coatings that can withstand long term extreme working conditions. New design approaches of multi-layer composite thermal barrier coating systems can adopt to the required trend of increasing working temperature of jet engines, mainly because of possibility of optimization of high-temperature durability and long lifetime as described in Li (2014) and in Zhou et al. (2003).

For proper selection of correct protecting materials, it is essential to understand the influence of high temperature exposure on oxidation of thermal barrier coatings. Many different microstructural changes, which lead up to the failure of protective coating, occur in TBCs during isothermal exposure. Ions of oxygen and water vapor can easily penetrate at high temperatures through the ceramic YSZ coating down to the metallic bond coat due to high ion conductivity of ceramic top coat. Oxygen ions are adsorbed by the MCrAlY bond coat and, subsequently, NiO, Al_2O_3 and Cr_2O_3 oxides are formed on the bond coat metallic surface. These oxides can react together and form spinel based on $Ni(Al,Cr)_2O_4$ which decreases cohesion and promotes initiation of microcracks at the bond coat/top coat interface. Diffusion of oxygen through ceramic coating can be limited by replacement of conventional YSZ top coat by nanocrystalline ceramic top coat, whose unique microstructure has the ability to act as a very effective oxygen diffusion barrier (Karlsson (2003), Daroonparvar (2013)).

Nomenclature

YSZ	Yttria Stabilized Zirconia
TBC	Thermal Barrier Coating
TGO	Thermally Grown Oxide

2. Materials and methods

All coatings were deposited by means of atmospheric plasma spraying utilizing a Sulzer Metco F4MB-XL gun mounted on an industrial 6-axis robot ABB IRB 2600. The substrates from Inconel Alloy 713LC superalloy were grit blasted using alumina abrasive particles, cleaned with ethanol in ultrasonic bath and dried with compressed air prior to the deposition. The conventional YSZ top coat was deposited from commercially available ZrO_2+7Y_2O_3 powder Amperit 831. The bond coat was of NiCoCrAlYHfSi type and was deposited using Amperit 405 powder. The experimental ceramic top was prepared from the mixture of YSZ and Mullite powder (71 vol. % of YSZ Amperit 831 and 29 vol. % of Metco 6150) and was deposited onto the ceramic YSZ interlayer prepared from Amperit 827 and bond coat prepared from Amperit 405. As-sprayed samples were isothermally heat treated at the temperatures of 1050, 1150, and 1250 °C for 50, 100, 200, 300, and 500 hours in a LT30 furnace (co. LAC). Heat treated samples were cut out using precise micro-cutting machine and cold mounted into the resin. Metallographic samples were grinded and polished according to modified process for thermal spray coatings sample preparation. Cross-sectional coatings' microstructure was observed by means of scanning electron microscopy using Tescan Lyra3 SEM equipped with Brucker EDAX analyzer. Phase transformations of both ceramic top coats (conventional and experimental TBCs) were evaluated using PANalytical Empyrean XRD. The growth of the TGO layer was investigated using the digital image analysis software ImageJ. The samples with the conventional YSZ top coat were labelled by the letter Y whereas the samples with the experimental Mullite-YSZ top coat were labelled by the letter M.

3. Results and discussion

The as-sprayed sample with the conventional TBC (Y0) consisted of the 160 μm thick bond coat, and the 350 μm thick top coat. The interface between the bond coat and the substrate was without the presence of apparent defects, such as cracks or pores. There was none thermally grown oxide at the interface between the top coat and the bond coat after spraying, see Fig. 1a, and aluminium, as an alloying element, remained stored in the bond coat, forming the intermetallic β-NiAl phase. The microstructure of ceramic YSZ top coat was characterized by the presence of small amount of vertical and horizontal micro-cracks and by porosity of about 17 %. In terms of phase composition, only metastable tetragonal YSZ phase (t'-YSZ) with the amount of 7.4 wt. % of Y_2O_3 was found after the deposition within the YSZ top coat. The experimental as-sprayed TBC (M0) consisted of the 180 μm thick bond coat, the 100 μm thick ceramic YSZ interlayer, and the 210 μm thick Mullite-YSZ top coat. Each individual layer of sample M0 met the

requirements for high quality interfaces. The bond coat/substrate interface was without apparent defects and copied the topography of blasted substrate surface. The interface between the bond coat and the ceramic interlayer was without defects and, again, matched the topography of the undelaying bond coat. The mullite-YSZ/interlayer interface is depicted by green line in Fig. 2a and, from the technological point of view, it represented smooth and imperceptible transition between the two materials. Microstructure of experimental top coat has lamellar morphology typical for APS deposition process. Based on the measured XRD diffraction patterns, the experimental Mullite-YSZ coating consisted of 58.9 wt. % metastable tetragonal YSZ phase (t'-YSZ), 2.6 wt. % cubic YSZ phase (c-YSZ), and 38.5 wt. % Mullite phase. The amount of Y_2O_3 was 6.8 wt. % in t'-YSZ and 3.7 wt. % in c-YSZ. The presence of cubic YSZ phase in as-sprayed experimental top coat has positive influence on decreasing the overall thermal conductivity of the ceramic coating (Brandt (1986)) and its presence in microstructure does not influence durability of the coating.

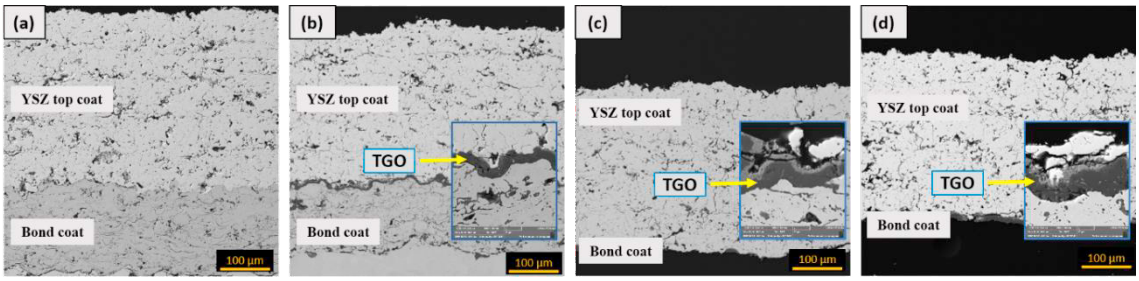

Fig. 1 Cross-sectional micrograph of conventional YSZ TBC: (a) as-sprayed, (b) after 500 hours at 1050 °C, (c) 500 hours at 1150 °C, and (d) 200 hours at 1250 °C; SEM-BSE.

The amorphous region in the experimental Mullite-YSZ system is apparent in Fig. 3a. This region has the length of approximately 10 µm and is located at the interface between the YSZ and the Mullite splats. Crystallization of nanoparticles in the form of dendritic structure, with the particle size of about 100 nm inside of the amorphous area, occurred during the deposition process. Formation of pure amorphous regions within the ceramic coating requires rapid solidification of molten splats after impacting the substrate of high thermal conductivity. Such conditions suppress the nucleation of crystalline phase during solidification (Song (2015)). The experimental Mullite-YSZ coating was deposited onto the ceramic interlayer with low thermal conductivity (0.85 W/mK), leading to very low cooling rates. Local overheating of the coating during multiple deposition passes resulted in crystallization of nanoparticles inside the amorphous areas.

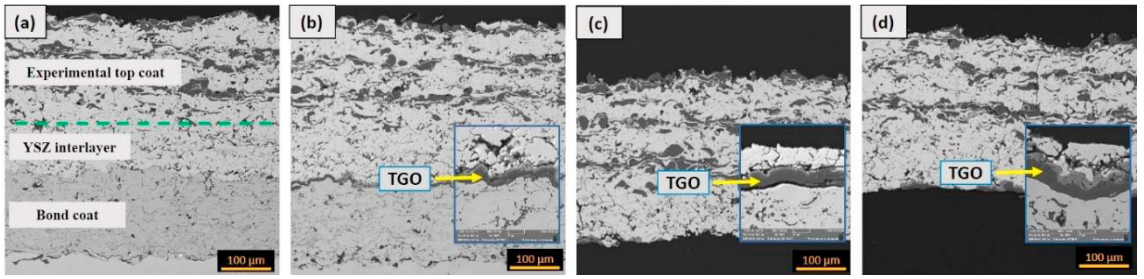

Fig. 2 Cross-sectional microstructure of experimental TBC: (a) as-sprayed, (b) after 500 hours at 1050 °C, (c) 500 hours at 1150 °C and (d) 200 hours at 1250 °C; SEM-BSE.

Isothermal oxidation of the conventional (see Fig. 1b) and experimental (see Fig. 2b) TBCs at 1050 °C for 500 hours did not lead to any microstructural changes within the ceramic top coat or the metallic bond coat. The dwell time of 500 hours at 1150 °C led to delamination of both TBCs at the bond coat/top coat interface due to the undesirable growth of thermally grown oxide. In the microstructure of YSZ top coat was found higher amount of vertical and horizontal micro-cracks compared to initial microstructure, see Fig. 1c. The same phenomenon was also observed for the Mullite-YSZ top coat, however, the amount of vertical microcracks was found to be significantly lower compared to initial state, see Fig. 2c. Isothermal oxidation at the temperature of 1250 °C led to delamination of both studied

TBCs after 200 hours, mainly because of the growth of the TGO layer at the bond coat/top coat interface. Furthermore, microstructural changes appeared in the ceramic top coat of both TBCs as well. In the conventional YSZ top coat, many vertical and horizontal micro-cracks were initiated at TC/BC interface due to stresses arising during growth of the TGO layer and/or inside of ceramic coating during cooling stresses related to different thermal expansions, see Fig. 1d. Horizontally oriented mullite phase in the experimental coating system serves as an effective barrier (based on crack bridging) to propagation of vertical microcracks, see Fig. 2d, and for that reason, the amount of cracks within the Mullite-YSZ coating is lower in comparison to the conventional YSZ coating. The microstructure of the amorphous areas in the experimental Mullite-YSZ coating after isothermal oxidation is shown in Fig. 3. It is seen that higher temperature and prolonged dwell time led to either nucleation of new particles inside the amorphous areas or growth in size of already present nanocrystalline particles. It is presumed, based on EDX analyses, that these nanoparticles are chemically based on ZrO_2. The long-term dwell time at higher temperatures led also to sintering of some of already formed nanoparticles, see Fig. 3c. Fine network structure of sintered ZrO_2 nanoparticles was formed during isothermal oxidation at 1250 °C for 200 hours, see Fig. 3d.

Fig. 3 Amorphous areas within experimental Mullite-YSZ coating: (a) as-sprayed, (b) after 500 hours at 1050 °C, (c) 500 hours at 1150 °C and

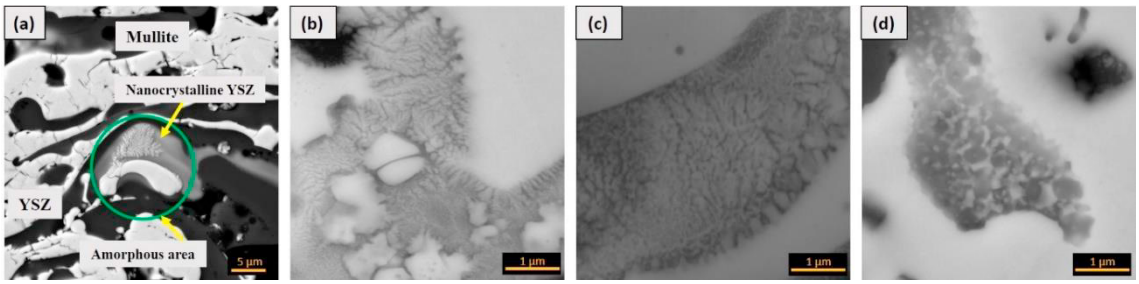

(d) 200 hours at 1250 °C; SEM-BSE.

Diffusion of oxygen through the ceramic coating during isothermal oxidation causes progressive oxidation of metallic bond coat. The dark oxide layer based on Al_2O_3 (TGO) is not formed only at the bond coat/top coat interface, but also inside the bond coat between the individual splats and/or in the vicinity of structural defects like pores, un-melted particles, etc. Other multicomponent oxides (spinel) based on Cr, Ni Co and Al are formed with increasing dwell time. Growth of thermally grown oxide based on Al_2O_3 together with spinel is one of the most important factors influencing overall structural integrity and life time of thermal barrier coatings. From the thermodynamic point of view, pure α-Al_2O_3 oxide is formed predominantly, due to its lowest free Gibbs energy (Liu (2016)).

The source of aluminium for formation of Al_2O_3 oxide is primarily intermetallic β-NiAl phase. As it is shown in Fig. 4a, the compact oxide layer with columnar structure and thickness of 2.95 µm was formed at the bond coat/top coat interface in the conventional TBC after isothermal oxidation at 1050 °C for 50 hours. In comparison, the thin Al_2O_3 oxide layer of thickness of 2.71 µm was formed in the experimental TBC after same thermal exposure.

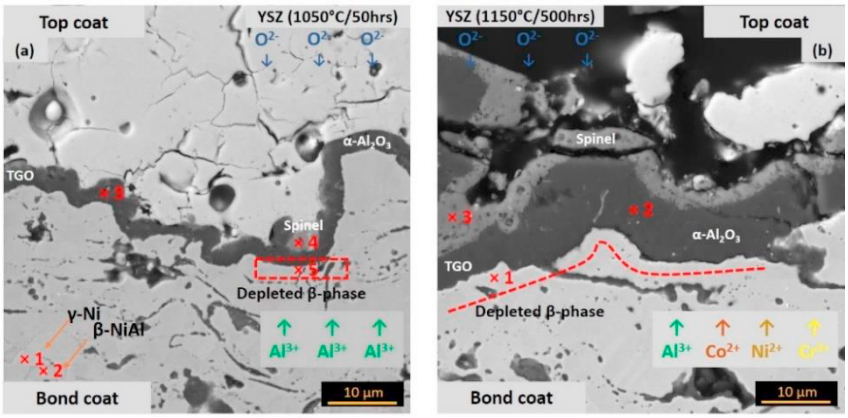

Fig. 4 Growth of thermally grown oxide after: (a) 50 hours at 1050 °C and (b) 500 hours at 1150 °C; SEM-BSE.

The EDX analyses confirmed that the compact columnar layer is stochiometric Al_2O_3 oxide, see Table 1. The local depletion of Al^{3+} in the immediate vicinity of the TGO/bond coat interface was caused by the growth of TGO. Once the content of Al^{3+} in β-NiAl phase is under critical level, the so called depleted β-phase is formed and formation of undesirable oxides rich in Cr and Ni occurs. Diffusion of oxygen at temperature of 1150 °C is accelerated because of higher activity and, therefore, growing of the TGO layer is faster. The thickness of the TGO layer in the case of the conventional TBC after 500 hours oxidation at 1150 °C was 12.51 μm, whereas the thickness of the TGO layer in the experimental TBC was 11.85 μm. The thermally grown oxide layer after long term high temperature exposure is not composed just of protective Al_2O_3 oxide, but also of porous undesirable oxides based on NiO, Cr_2O_3 and/or (Ni, Co)(Al, Cr)$_2O_4$ spinel (Eriksson (2011)). Progressive growing of the TGO layer increases the stresses at the top coat/TGO interface, which causes initiation and propagation of microcracks. The overall failure of TBCs coating caused by delamination is the result of coalescence of microcracks followed by initiation of magistral crack and its propagation at and near the top coat/TGO interface. The critical thickness of TGO which caused delamination of ceramic top coat after 100 hours at 1150 °C was 5.7 μm in case of conventional YSZ coating and 9.6 μm after 300 hours at 1150 °C in case of experimental Mullite-YSZ coating.

Table 1. EDS analyses of thermally grown oxide [wt. %].

Sample/point		Ni	Co	Cr	Al	O	Description
Y1	1	56.3	20.0	18.1	5.6	-	γ-Ni phase
	2	67.1	10.9	5.7	16.3	-	β-NiAl phase
	3	-	-	-	59.6	40.4	TGO (α-Al_2O_3)
	4	17.6	16.1	27.0	15.5	23.8	TGO (spinel)
	5	64.4	13.9	16.3	5.4	-	Depleted β-phase
Y10	1	64.9	14.4	16.1	4.6	-	Depleted β-phase
	2	-	-	-	59.8	40.2	TGO (α-Al_2O_3)
	3	19.4	8.9	3.4	35.6	32.7	TGO (spinel)

During isothermal oxidation at the temperature of 1050 °C, the initial metastable tetragonal YSZ phase (100 wt. %) in conventional YSZ was decomposed into the stable tetragonal YSZ phase (t-YSZ) and cubic YSZ phase. As it is shown in Table 2, with increasing time and temperature, the amount of tetragonal YSZ phase decreases whereas the amount of cubic YSZ phase increases. The content of Y_2O_3 within the t-YSZ phase changes from the initial value of 7.4 wt. % to 5.9 wt. % after 200 hours at 1250 °C. This reduction was compensated by increasing Y_2O_3 content in c-YSZ, from 4.2 wt. % after 500 hours at 1050 °C, up to 10.5 wt. % after 200 hours at 1250 °C. The long-term exposure at 1150 °C led to transformation of t-YSZ with low content of Y_2O_3 to undesirable monoclinic YSZ phase during cooling.

Table 2. Phase composition of YSZ and Mullite-YSZ samples after isothermal oxidation.

			Phases [wt. %]				Y_2O_3 [wt. %]	
Temp [°C]	Hours	Sample	t-YSZ	c-YSZ	m-YSZ	Mullite	c-YSZ	t-YSZ
As-sprayed		Y0	100	-	-	-	-	7.4
1050	500	Y5	87	13	-	-	4.2	6.0
1150	500	Y10	83	12	5	-	7.5	6.0
1250	200	Y13	77	22	1	-	10.5	5.9
As-sprayed		M0	58.9	2.6	-	38.5	6.8	3.7
1050	500	M5	37	7	-	56	6.4	6.0
1150	500	M10	37	7	-	56	8.2	6.0
1250	200	M13	30	13	-	57	10.1	5.2

During isothermal oxidation of the experimental Mullite-YSZ coating at 1050 °C, the initial content of mullite phase increased from 38.5 wt. % up to 56 wt. %. The metastable amorphous phase underwent transformation to stable crystalline phase above 970 °C (Kriven (2001)). As previously, increasing time and temperature led to transformation of metastable tetragonal YSZ phase to stable t-YSZ phase in the Mullite-YSZ coating. The content of the c-YSZ phase

increased with increasing dwell time and temperature, whereas the content of the mullite phase did not change and was found independent of both the dwell time and temperature. There was also no presence of the undesirable monoclinic YSZ phase. Diffusion of Y_2O_3 from t-YSZ to c-YSZ was reduced by the presence of mullite phase and for that reason, the transformation from t-YSZ with low content of Y_2O_3 to m-YSZ did not proceed during the cooling period.

4. Conclusions

Isothermal oxidation at the temperature of 1050 °C for 500 hours did not lead to the failure of studied TBCs, both the conventional and experimental thermal barrier coatings retained their integrity. Oxidation at the temperature of 1150 °C caused the failure of the conventional TBC after 100 hours, whereas the experimental Mullite-YSZ coating withstood 200 hours without failure. The thickness and microstructure of thermally grown oxide had significant impact on the lifetime and structural integrity of TBCs. In all tests, the measured thickness of the TGO layer was lower for the experimental Mullite-YSZ TBC than for the conventional YSZ TBC. Nucleation and growing of nanocrystalline t-ZrO_2 phase in the amorphous areas present within the experimental top coat occurred above the temperature of 970 °C. Oxidation of the conventional YSZ TBCs at the temperatures of 1150 and 1250 °C led to the formation of detrimental monoclinic YSZ phase within the ceramic top coat whereas no m-YSZ phase was detected in the experimental Mullite-YSZ top coat.

Acknowledgements

The research was carried out under the project Research Center of Surface Treatment TE02000011 with financial support from the Technology Agency of the Czech Republic.

References

Brandt, R., Pawlowski, L., Neuer, G. 1968. Specific heat and thermal conductivity of plasma sprayed yttria-stabilized zirconia and NiAl, NiCr, NiCrAl, NiCrAlY, NiCoCrAlY coatings. High Temperatures-High Pressures 18(1), 65-77.

Daroonparvar, M., Aziz Mat Yajid, M., Yusof, N.M., Sakhataw Hussain, M., 2013. Improved Thermally Grown Oxide Scale in Air Plasma Sprayed NiCrAlY/Nano-YSZ Coatings. Journal of Nanomaterials 203, 1-9.

Eriksson, R., Brodin, H., Johansson, S., Ostergren, L., Li, X., 2011. Influence of isothermal and cyclic heat treatments on adhesion of plasma sprayed thermal barrier coatings. Surface and Coatings Technology 205, 5422-5429.

Karlsson, A.M., Hutchinson, J.W., Evans, A.G., 2003. The displacement of the thermally grown oxide in thermal barrier systems upon temperature cycling. Materials Science and Engineering A 351, 244-257.

Kriven, W., 2001. Crystallization Mechanism of Amorphous Mullite and the Al2O3-SiO2 Phase Diagram. MRS Proceedings 702, 831-837.

Li, X. 2014. Cyclic and Isothermal Oxidation Resistance of ASPS Thermal Barrier Coating Systems. Master Thesis, Canada.

Liu, X., Wang, T., Li, C., Zheng, Z., Li, O., 2016. Microstructural evolution and growth kinetics of thermally grown oxides in plasma sprayed thermal barrier coatings. Progress in Natural Science: Materials Interaction 26, 103-111.

Song, X., Suhonen, T., Sun, C., Huang, L., Zheng, X., Zeng, Y., 2015. Microstructures, microhardness, and crystallization behaviours of amorphous Al2O3-YSZ coatings prepared by air plasma spraying. Surface Review and Letters 22, 9-15.

Zhou, C., Yu, J., Gong, S., Xu, H., 2003. Influence of water vapor on the high temperature oxidation behaviour of thermal barrier coatings. Materials Science and Engineering: A 348, 327-332.